Electronic Supplementary Material (ESI) for New Journal of Chemistry.

A zinc^{2+}-dpbt framework: a luminescence sensing of Cu^{2+}, Ag^{+} MnO_4^{-} and Cr(VI) ($Cr_2O_7^{2-}$ and CrO_4^{2-}) ions †

Yan Cao,[a] Yan Zhang,[a] Liang-wei Gu,[a] Xing-mei Qin,[a] Hai-Ye Li,[*b] He-Dong Bian,[a] Han-Fu Liu,[a] Fu-Ping Huang[*a]

Real environmental samples preparation

The reproducibility of **1** for sensing Cu^{2+} and Ag^{+} was also measured. After the first quenching experiment, the test material of **1** was recollected by centrifugation and washed several times with deionized water. The regenerated **1** was used again in the detection experiments and the fluorescence emission intensities were measured.

Table S1 Selected Bond Lengths (Å) and Angles (°) for **1**

Symmetry codes: (A) -x+1/3, -y+2/3, -z+5/3; (B) y-1/3, -x+y+1/3, -z+4/3; (C) x-y+2/3, x+1/3, -z+4/3.			
Zn1—Cl1	2.3144 (8)	Zn1B—Cl1	2.5059 (8)
Zn1—N1	2.291 (2)	Zn1—N2	2.015 (2)
Zn1C—N4	2.023 (2)	Zn1—Cl1C	2.5058 (8)
Zn1—N4B	2.023 (2)		
Cl1—Zn1—Cl1C	102.23 (4)	N1—Zn1—Cl1	98.95 (7)
N1—Zn1—Cl1C	156.51 (6)	N2—Zn1—Cl1	112.93 (7)
N2—Zn1—Cl1C	87.83 (6)	N2—Zn1—N1	74.54 (8)
N2—Zn1—N4B	148.99 (9)	N4B—Zn1—Cl1	96.84 (6)
N4B—Zn1—Cl1C	94.38 (7)	N4B—Zn1—N1	93.08 (9)

[*a] *State Key Laboratory for the Chemistry and Molecular Engineering of Medicinal Resources, School of Chemistry and Pharmacy, Guangxi Normal University, Guilin, 541004, P. R. China. E-mail: huangfp2010@163.com*

[*b] *School of Chemistry and Pharmacy, Guangxi Normal University, Guilin, 541004, P. R. China. E-mail: lihaiye2010@163.com*

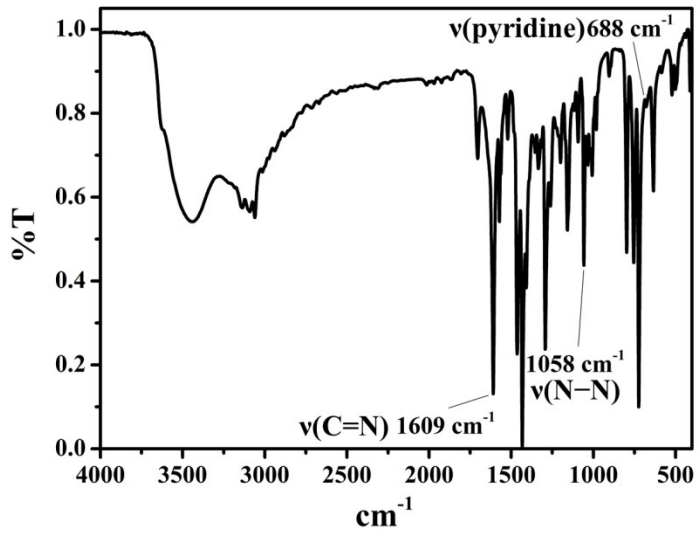

Fig. S1 IR spectra of complex **1**.

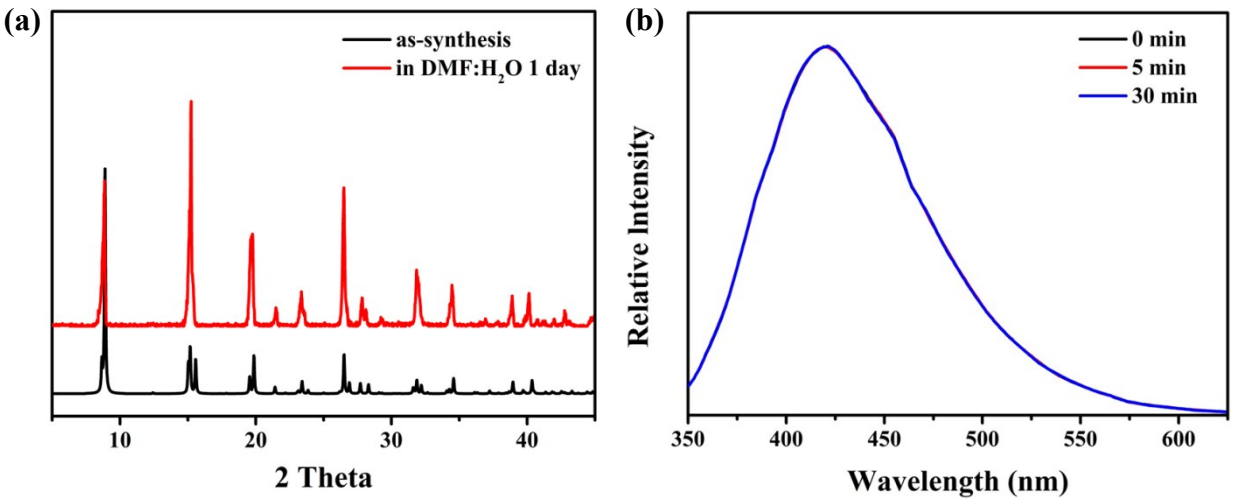

Fig. S2 (a) Complex **1** was placed in DMF: H_2O(V/V=1:1) solutions for 1day of PXRD patterns. (b) Fluorescence measurements of **1** immersed into the DMF: H_2O(V/V=1:1) solutions as the suspensions for 0 min and after 30 min.

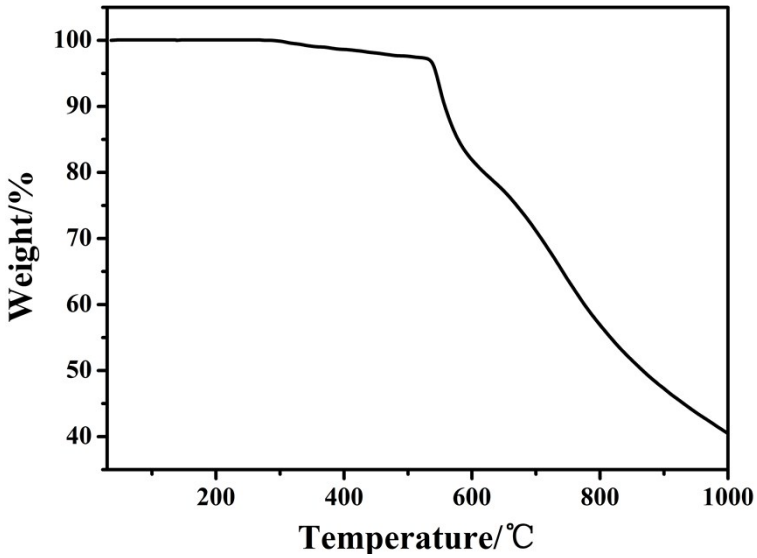

Fig. S3 TGA curve of **1**.

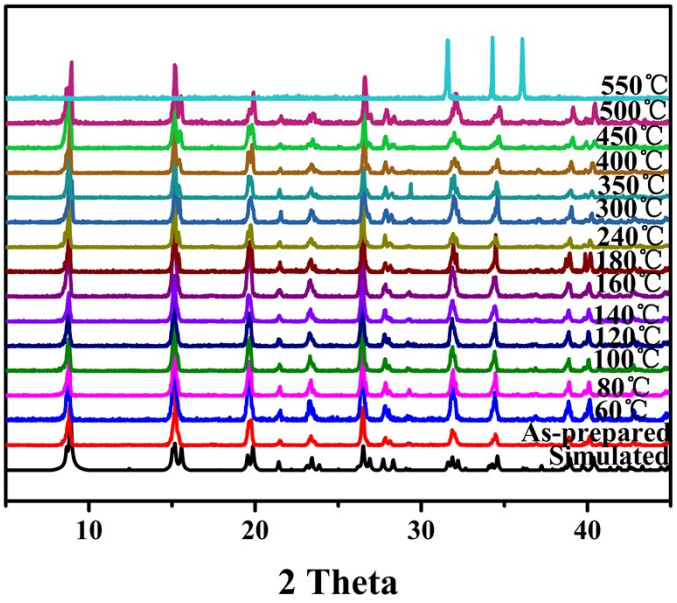

Fig. S4 PXRD patterns of **1** at different temperatures and the simulated one calculated from the single crystal structure analysis.

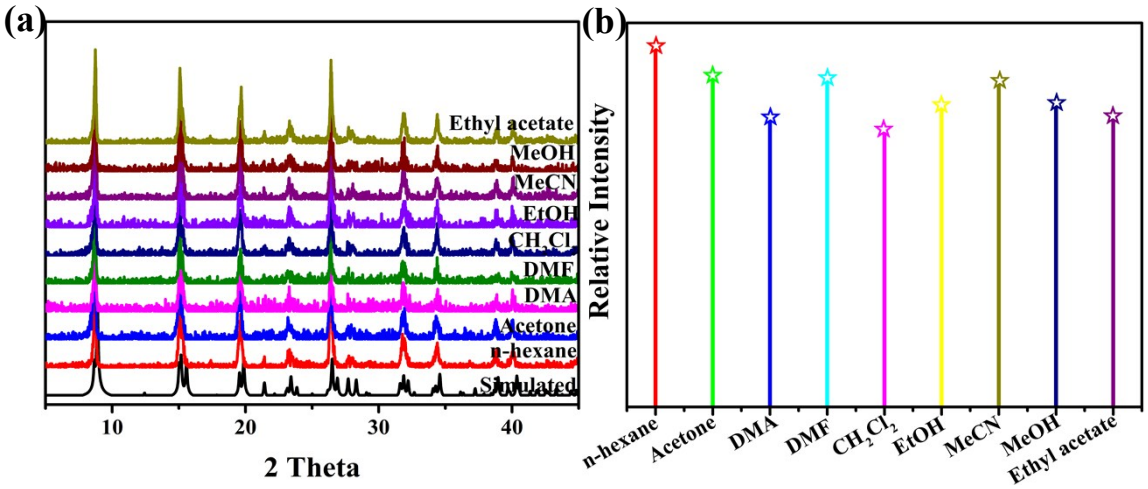

Fig. S5 The PXRD patterns of **1** treated in different solvents.(a) Fluorescence measurements of **1** in various pure solvents. (b)

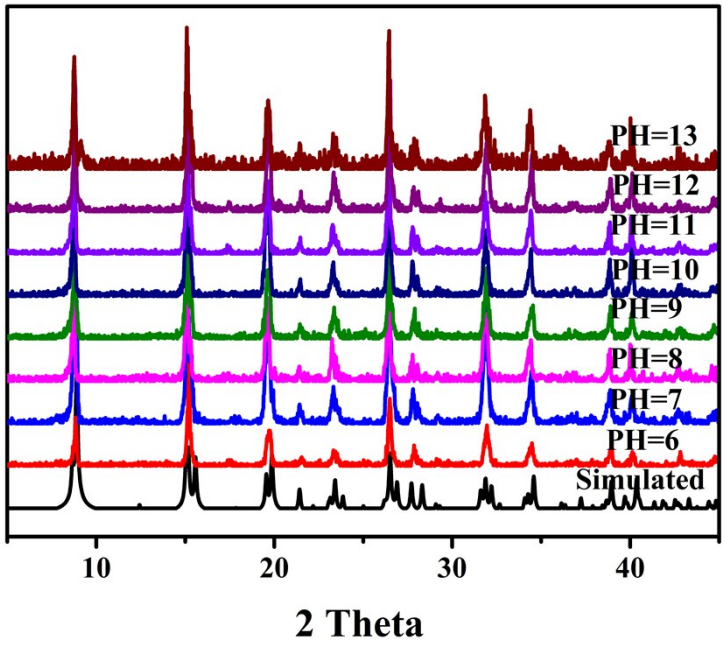

Fig. S6. PXRD patterns of **1** in different pH values in the range of 6-13.

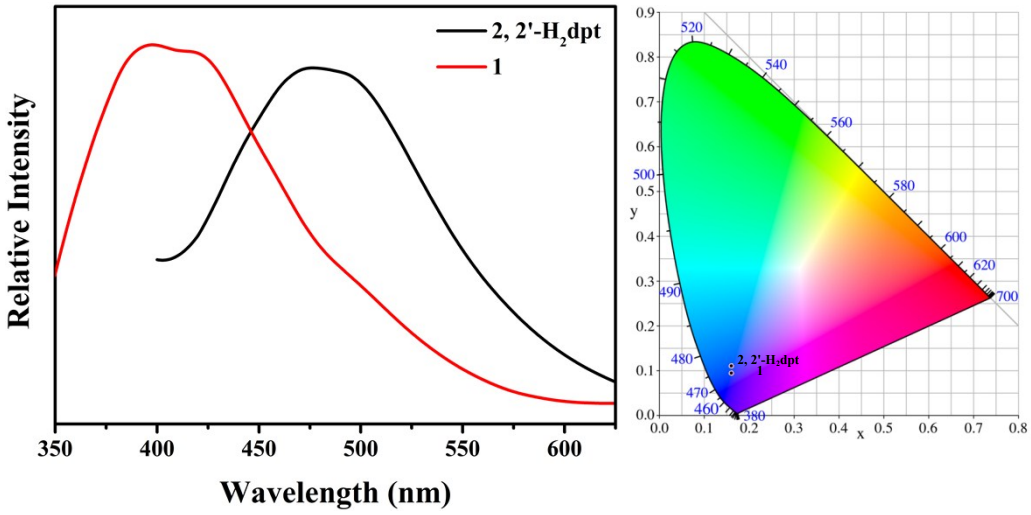

Fig. S7 The solid luminescent emissions of ligand 2,2′-H_2dbpt and **1**.

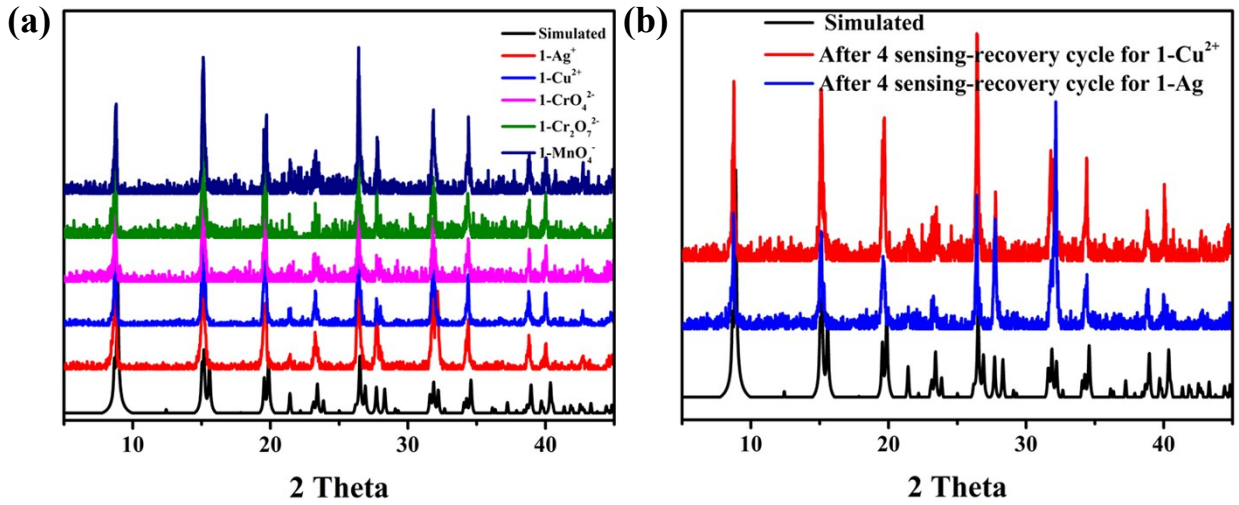

Fig. S8 **(a)** Powder X-ray diffraction patterns of the activated framework, and diffraction patterns obtained after the introduction of various metal ions: **1**-Cu^{2+}, **1**-Ag^{+}, **1**-MnO_4^-, **1**-$Cr_2O_7^{2-}$ and **1**-CrO_4^{2-} .(b) PXRD curves of **1**after four sensing recovery cycles for Ag^{+} and Cu^{2+} ions showing that structural integrity of the framework is maintained.

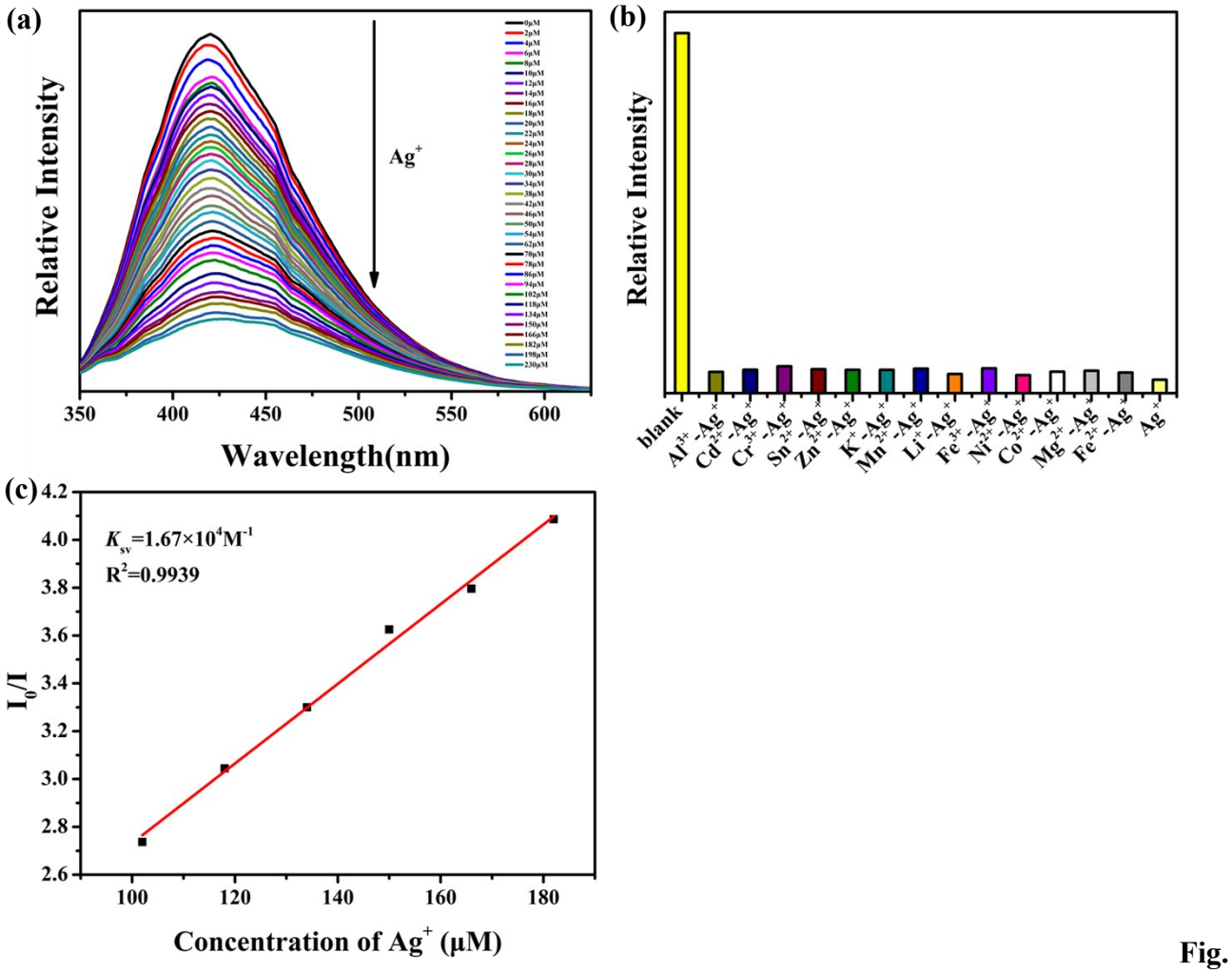

Fig. S9 (a) Emission spectra of **1** dispersed in DMF: H_2O(V/V=1:1) solution with different

concentrations of Ag^+. (b) Emission spectra of **1** dispersed in DMF: H_2O(V/V=1:1) solution with different concentrations of Ag^+. (c) The Stern–Volmer plot of I_0/I versus Ag^+ concentration.

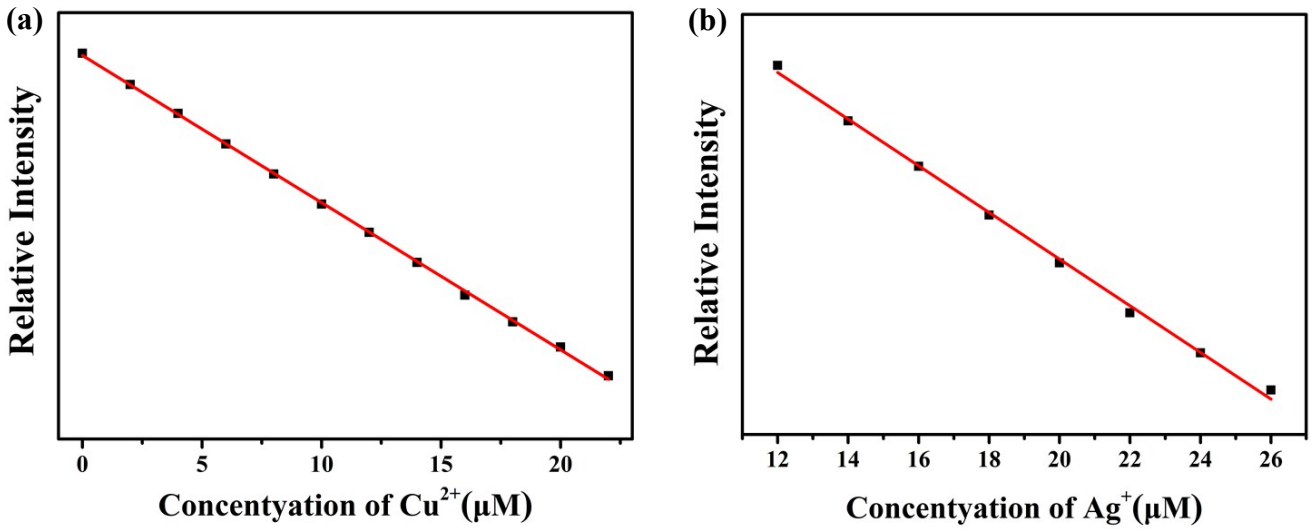

Fig. S10 Linear region of fluorescence intensity of **1** in DMF: H_2O(V/V=1:1) solution upon addition of Cu^{2+} (a) and Ag^+ (b).

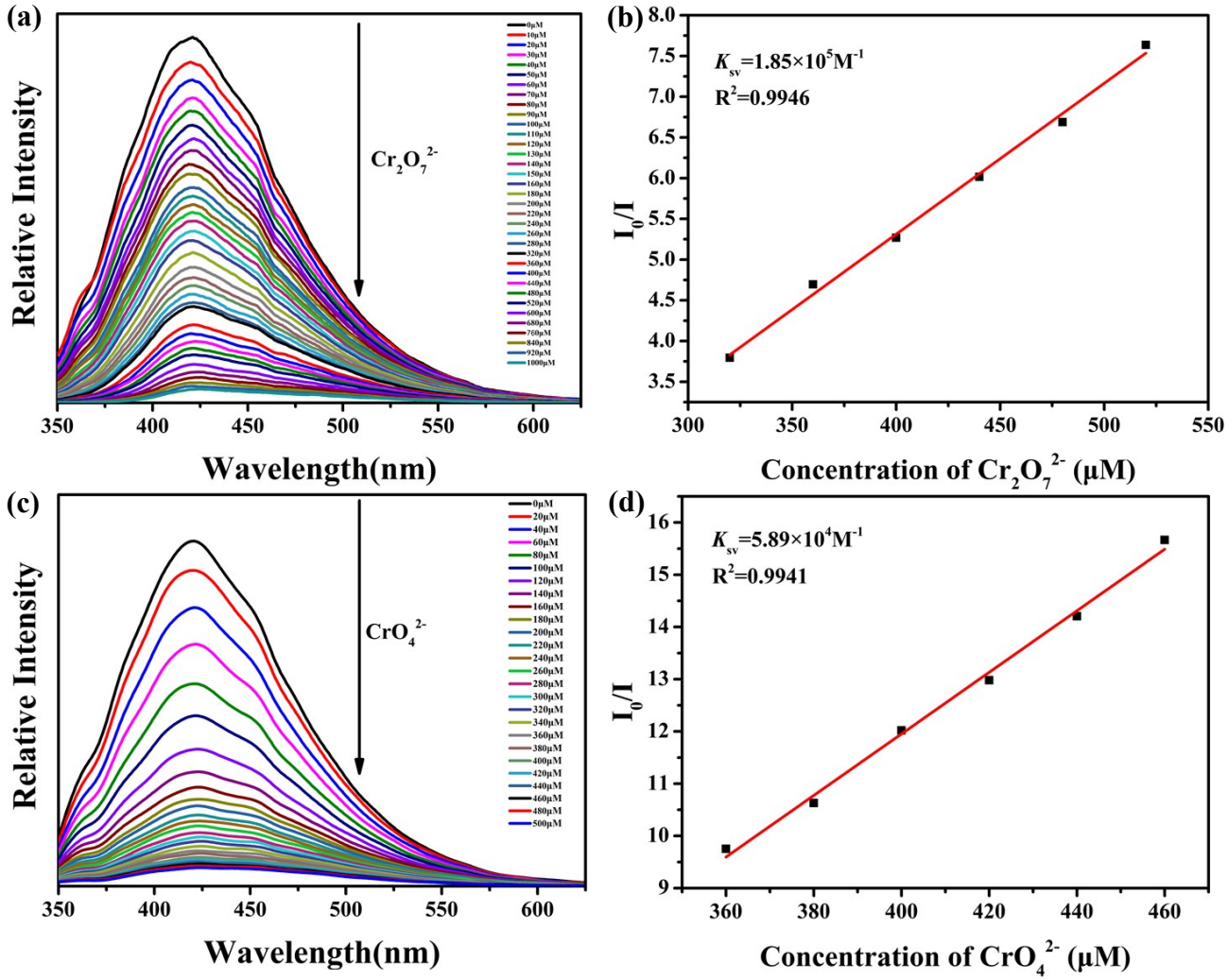

Fig. S11 (a) Emission spectra of **1** dispersed in DMF: H_2O(V/V=1:1) solution with different concentrations of $Cr_2O_7^{2-}$. (b) The Stern–Volmer plot of I_0/I versus $Cr_2O_7^{2-}$ concentration. (c) Emission spectra of **1** dispersed in DMF: H_2O(V/V=1:1) solution with different concentrations of CrO_4^{2-}. (d) The Stern–Volmer plot of I_0/I versus CrO_4^{2-} concentration.

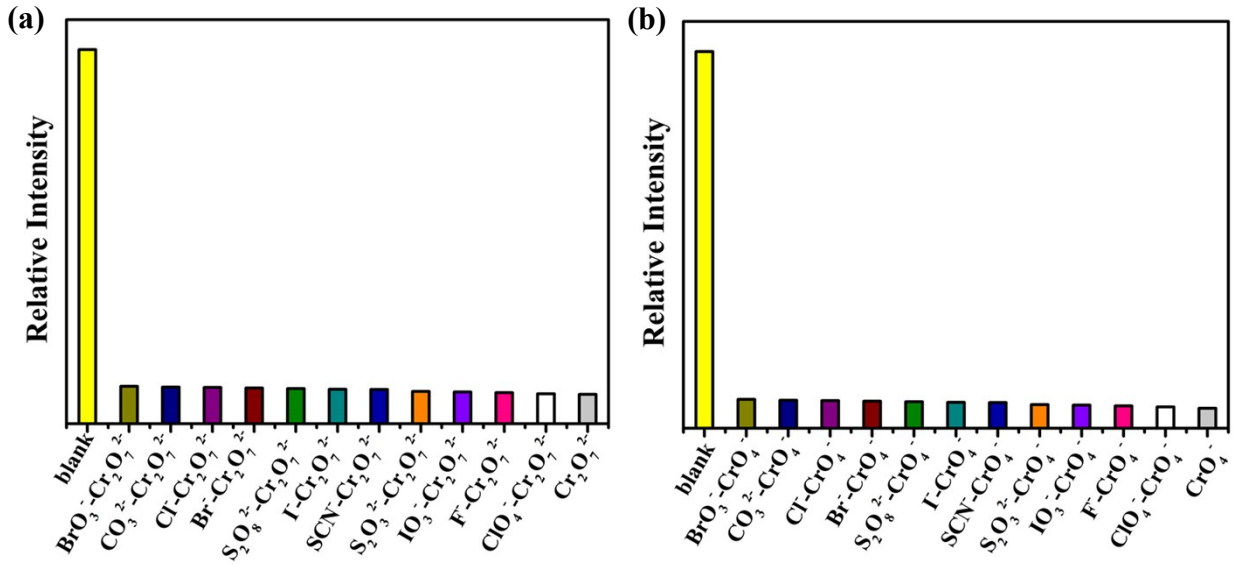

Fig. S12 (a) Luminescence intensity of the **1** dispersed in a mixture of other anions with $Cr_2O_7^{2-}$ (a) and CrO_4^{2-} (b).

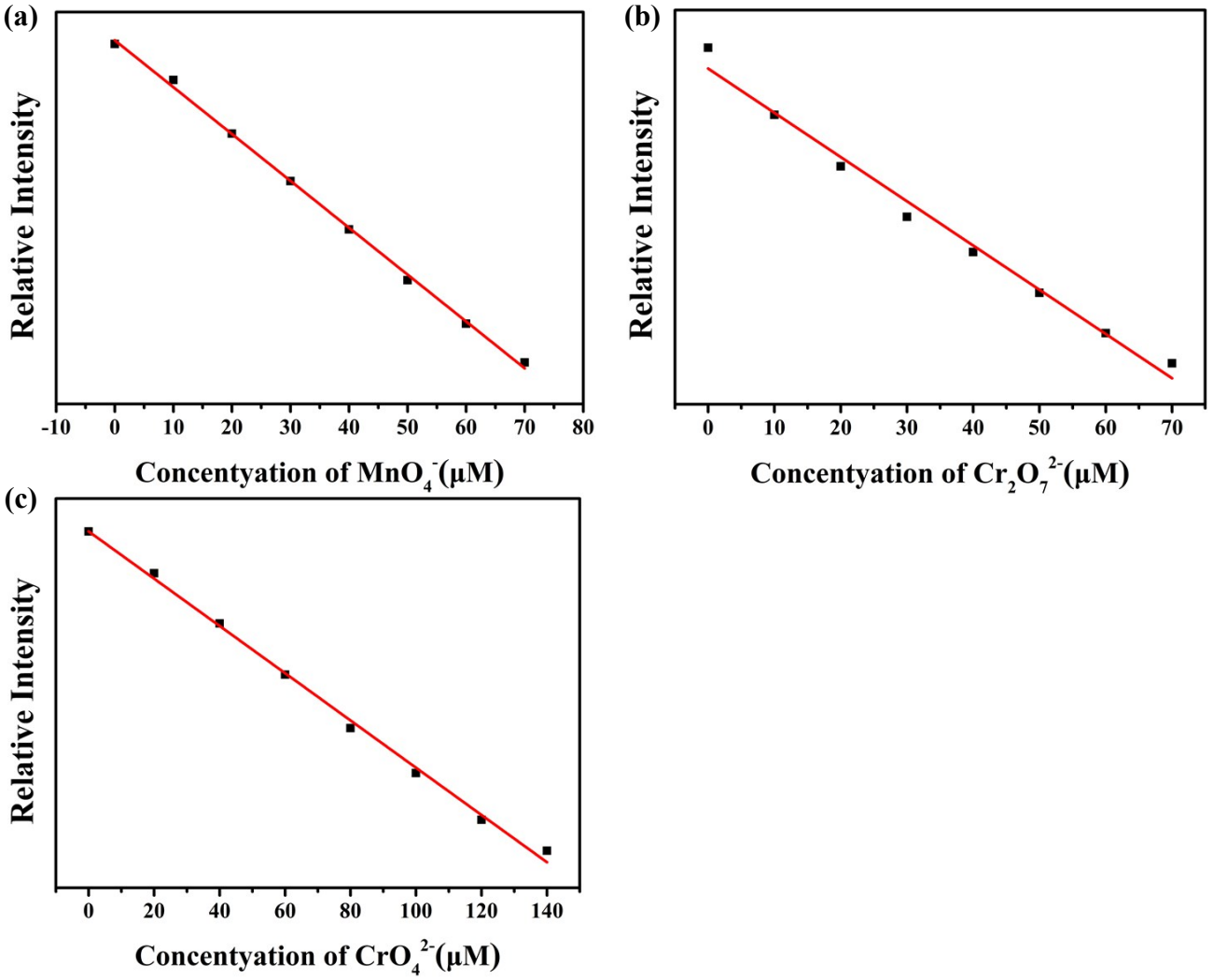

Fig. S13 Linear region of fluorescence intensity of **1** in DMF: H_2O(V/V=1:1) solution upon addition of MnO_4^- (a), $Cr_2O_7^{2-}$ (b) and CrO_4^{2-} (c).

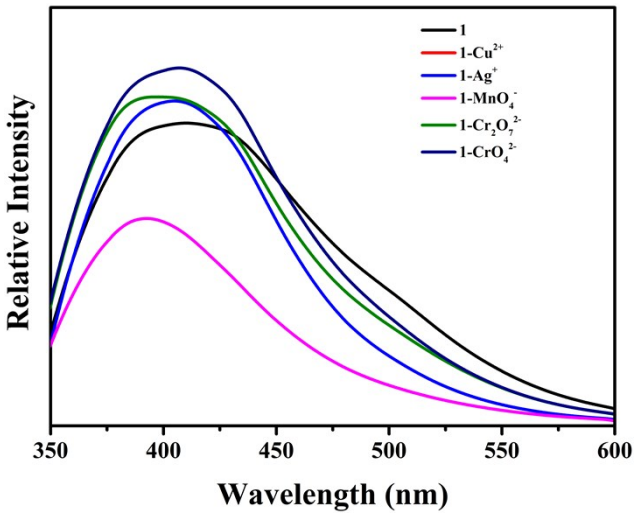

Fig. S14 Emission spectra of **1**, **1**-Cu^{2+}, **1**-Ag^+, **1**-MnO_4^-, **1**-$Cr_2O_7^{2-}$ and **1**-CrO_4^{2-} in solid state at room temperature.

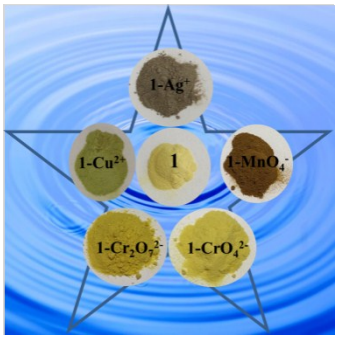

Fig. S15 The photographs of **1**-M^{n+} (M= Cu^{2+}, Ag^{+}, MnO_4^- and Cr(VI)($Cr_2O_7^{2-}$ and CrO_4^{2-}), respectively) as solid.

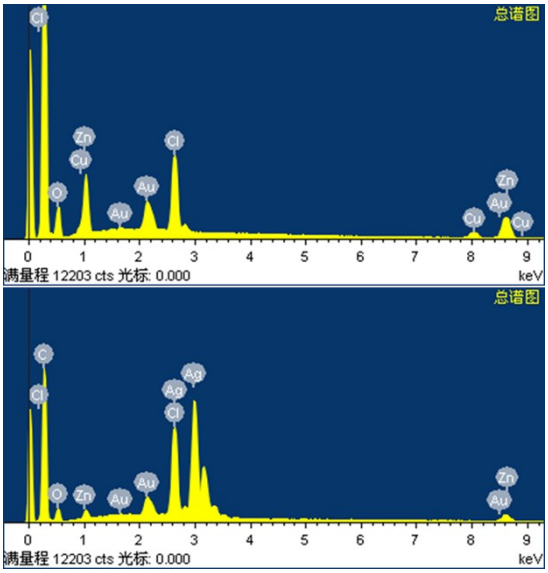

Fig. S16 EDS spectrum of **1**-Cu^{2+} and **1**-Ag^{+}.

Table S2 ICP-MS analysis results for Cu^{2+} and Ag^{+} included **1**.

Complex	Zn^{2+} Content (%)	Cu^{2+} Content (%)	Ag^{+} Content (%)
1-Cu^{2+}	35.68	6.31	
1-Ag^{+}	27.47		37.84

Table S3. K_{sv} and LOD of MOF-based luminescent sensors for Cu^{2+}, Ag^{+}, MnO_4^-, $Cr_2O_7^{2-}$ and CrO_4^{2-}.

MOF-based fluorescent materials	Analyte	Detection limits	Quenching constant (M^{-1})	Recyclability	Solvent	Ref
$Cd_2(L_3)(DMF)_2$(Cd-MOF-74)	Cu^{2+}	78.7*u*M	1806	NO	Water	1
$[Cd(L)_2]\cdot(DMF)_{0.92}$	Cu^{2+}	3.9ppm	4.4×10^3	YES	DMF	2
$\{[Eu_2K_2(L_1)_2(H_2O)_6]\cdot5H_2O\}_n$	Cu^{2+}	10^{-6}M	5.2×10^4	NO	Ethanol	3
$Zr_6O_4(OH)_4(L_2\text{-}H_2)_3$	Cu^{2+}	67nM	4.5×10^5		Water	4
$\{Zn_5(L)_2(DMF)_2(\mu_3\text{-}H_2O)]\cdot2DMF\}$	Cu^{2+}	1.01ppm	1.10×10^3	NO	DMF	5

	Ag^{+}	0.64 ppm	2.24×10^{3}	NO	DMF	
$EuC_{12}H_{10}Br_6O_{11}$	Cu^{2+}	7.52×10^{-5}M	4612.0	YES	Ethanol	6
$[Cd(L)(TPOM)_{0.75}]\cdot xS$	Cu^{2+}		17890	YES	Water	7
$[Zn(L)(BBI)\cdot(H_2O)_2]$	$Cr_2O_7^{2-}$		11680			
$[Cd(L)(TPOM)_{0.75}]\cdot xS$	$Cr_2O_7^{2-}$		13450			
$[Eu_6Zn_6(L_2)_2(L_3)_2O_2(OAc)_{18}]$	Ag^{+}	7.59 μM	32520	NO	DMF	8
$[Eu_6Zn_6(L_2)_2(L_3)_2O_2(OAc)_{18}]$	Ag^{+}	2.26 μM	32520	NO	DMF	9
$\{[Co_2(C_{17}H_8O_8)(C_{14}H_{14}N_4)_2]\cdot3H_2O\}_n$	Ag^{+}	23nM	3.4×10^{5}	NO	Water	10
$\{[Tb_2(L)_2(H_2O)_2]_n\cdot(5H_2O)\cdot(6DMAC)\}_n$	MnO_4^{-}	4.48×10^{-5} mM	1200	YES	Water	11
$\{[Eu_2(L)_2(H_2O)_2]_n\cdot(5H_2O)\cdot(6DMAC)\}_n$	$Cr_2O_7^{2-}$	8.94×10^{-5} M	1052			
$[Cd(L)_2(H_2O)_2]_n$	MnO_4^{-}	1.73×10^{-4} M	2.2×10^{4}	NO	Water	12
	$Cr_2O_7^{2-}$	1.75×10^{-4} M	1.1×10^{4}			
	CrO_4^{2-}	3.41×10^{-5} M	5.1×10^{4}	NO		
$\{[Eu(L)(H_2O)_2]\cdot5H_2O\}_n$	MnO_4^{-}		0.51×10^{3}	NO	Water	13
	$Cr_2O_7^{2-}$		1.36×10^{3}			
	CrO_4^{2-}		1.74×10^{3}			
$[Cd_3(bpe)_2(ceba)_2(fa)_2(H_2O)_2]_n$	$Cr_2O_7^{2-}$		9510	NO	Water	14
$[Eu_2(tpbpc)_4\cdot CO_3\cdot4H_2O]\cdot DMF$	$Cr_2O_7^{2-}$	1.07ppm	1.04×10^{4}	YES	Water	15
	CrO_4^{2-}	0.33ppm	4.85×10^{3}	YES		
$\{[Zn(btz)]_n\}$	$Cr_2O_7^{2-}$	2×10^{-6} M	4.23×10^{3}	YES	Water	16
$\{[Zn(btz)]_n\}$	CrO_4^{2-}	10^{-5} M	3.19×10^{3}			
$\{[Zn_2(ttz)H_2O]_n\}$	$Cr_2O_7^{2-}$	2×10^{-5} M	2.19×10^{3}			
$\{[Zn_2(ttz)H_2O]_n\}$	CrO_4^{2-}	2×10^{-5} M	2.35×10^{3}			
$\{[Zn_3(L)(OH)(H_2O)_5]\cdot NMP\cdot2H_2O\}_n$	MnO_4^{-}	3.38×10^{-4} M	1.1×10^{4}	YES	Water	17
$\{[Zn_3(L)(OH)(H_2O)_5]\cdot NMP\cdot2H_2O\}_n$	$Cr_2O_7^{2-}$	6.05×10^{-5} M	6.6×10^{4}			
$\{[Zn_3(L)(OH)(H_2O)_5]\cdot NMP\cdot2H_2O\}_n$	CrO_4^{2-}	4.29×10^{-4} M	1.3×10^{4}			
$\{[Zn_6Cl_6(2,2'\text{-dbpt})_3]\cdot2H_2O\}_n$	Cu^{2+}	0.73μM	5.96×10^{4}	NO	Water	This work
	Ag^{+}	6.40μM	1.67×10^{4}			
	MnO_4^{-}	6.14μM	2×10^{5}			
	$Cr_2O_7^{2-}$	13.64μM	1.85×10^{5}			
	CrO_4^{2-}	12.33μM	5.89×10^{4}			

References

1A. J. Howarth, T. C. Wang, S. S. Al-Juaid, S. G. Aziz, J. T. Hupp and O. K. Farha, *Dalton Trans.*, 2016, **45**, 93–97.

2S. Senthilkumar, R. Goswami, V. J. Smith, H. C. Bajaj and S. Neogi, *ACS Sustainable Chem. Eng.*, 2018, **6**, 10295–10306.

3H. Zhang, R. Fan, W. Chen, J. Fan, Y. Dong, Y. Song, X. Du, P. Wang and Y. Yang, *Crystal Growth & Design*, 2016, **16**, 5429–5440.

4M. R. Cerón, M. Izquierdo, N. Alegret, J. A. Valdez, A. Rodríguez-Fortea, M. M. Olmstead, A. L. Balch, J. M. Poblet and L. Echegoyen, *Chem. Commun.*, 2016, **52**, 64–67.

5J.-C. Jin, X.-R. Wu, Z.-D. Luo, F.-Y. Deng, J.-Q. Liu, A. Singh and A. Kumar, *CrystEngComm*, 2017, **19**, 4368–4377.

6J. A. Smith, M. A. Singh-Wilmot, K. P. Carter, C. L. Cahill and J. A. Ridenour, *Crystal Growth & Design*, 2019, **19**, 305–319.

7Y. Zhao, X. Xu, L. Qiu, X. Kang, L. Wen and B. Zhang, *ACS Appl. Mater. Interfaces*, 2017, **9**, 15164–15175.

8D. Jiang, X. Yang, H. Chen, F. Wang, S. Wang, T. Zhu, L. Zhang and S. Huang, *Dalton Trans.*, 2019, **48**, 2206–2212.

9D. Jiang, X. Yang, H. Chen, F. Wang, S. Wang, T. Zhu, L. Zhang and S. Huang, *Dalton Trans.*, 2019, **48**, 2206–2212.

10 Y. Liu, F. Zhang, P. Wu, C. Deng, Q. Yang, J. Xue, Y. Shi and J. Wang, *Inorg. Chem.*, 2019, **58**, 924–931.

11 L. (Leo) Liu, D. Zhu, L. L. Cao and D. W. Stephan, *Dalton Trans.*, 2017, **46**, 3095–3099.

12 Y.-T. Yan, F. Cao, W.-Y. Zhang, S.-S. Zhang, F. Zhang and Y.-Y. Wang, *New J. Chem.*, 2018, **42**, 9865–9875.

13 P.-F. Zhang, G.-P. Yang, G.-P. Li, F. Yang, W.-N. Liu, J.-Y. Li and Y.-Y. Wang, *Inorg. Chem.*, 2019, **58**, 13969–13978.

14 R.-R. Zhu, T. Wang, T. Yan, L. Jia, Z. Xue, J. Zhou, L. Du and Q.-H. Zhao, *Dalton Trans.*, 2019, **48**, 12159–12167.

15 J. Liu, G. Ji, J. Xiao and Z. Liu, *Inorg. Chem.*, 2017, **56**, 4197–4205.

16 C.-S. Cao, H.-C. Hu, H. Xu, W.-Z. Qiao, B. Zhao, *CrystEngComm*, 2016, **18**, 4445–4451.

17 Y. Zhao, X. Xu, L. Qiu, X. Kang, L. Wen and B. Zhang, *ACS Appl. Mater. Interfaces*, 2017, **9**, 15164–15175.